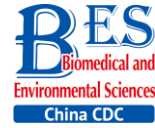


Original Article



Connexin43 Modulates X-Ray-Induced Pyroptosis in Human Umbilical Vein Endothelial Cells*

LI Chen¹, TIAN Mei¹, GOU Qiao¹, JIA Yong Rui², and SU Xu^{1, #}

1. China CDC Key Laboratory of Radiological Protection and Nuclear Emergency, National Institute for Radiological Protection, Chinese Center for Disease Control and Prevention, Beijing 100088, China; 2. Medical and Health Analysis Center, Peking University, Beijing 100191, China

Abstract

Objective Pyroptosis is an inflammatory form of programmed cell death. This phenomenon has been recently reported to play an important role in radiation-induced normal tissue injury. Connexin43 (Cx43) is a gap junction protein that regulates cell growth and apoptosis. In this study, we investigated the effect of Cx43 on X-ray-induced pyroptosis in the human umbilical vein endothelial cells (HUVECs).

Methods HUVECs, Cx43 overexpression, and Cx43 knockdown strains were irradiated with 10 Gy. Proteins were detected using western blot analysis. Cell pyroptosis was evaluated using the fluorescence-labeled inhibitor of caspase assay (FLICA) and propidium iodide staining through flow cytometry and confocal microscopy. Cell morphology and cytotoxicity were detected by scanning electron microscopy and lactate dehydrogenase release assay, respectively.

Results Irradiation with 10 Gy X-ray induced pyroptosis in the HUVECs and reduced Cx43 expression. The pyroptosis in the HUVECs was significantly attenuated by overexpression of Cx43 as it decreased the level of active caspase-1. However, interference of Cx43 expression with siRNA significantly promoted pyroptosis by increasing the active caspase-1 level. Pannexin1 (Panx1), a gap junction protein regulates pyroptosis, and its cleaved form is used to evaluate channel opening and active state. The level of cleaved Panx1 in the HUVECs and Cx43 knockdown strains increased in the presence of X-ray, but decreased in the Cx43 overexpression strains. Furthermore, interference of Panx1 with siRNA alleviated the upregulation of pyroptosis caused by Cx43 knockdown.

Conclusion Results suggest that single high-dose X-ray irradiation induces pyroptosis in the HUVECs. In addition, Cx43 regulates pyroptosis directly by activating caspase-1 or indirectly by cleaving Panx1.

Key words: X-ray; Connexin43; HUVECs; Pyroptosis

Biomed Environ Sci, 2019; 32(3): 177-188

doi: 10.3967/bes2019.025

ISSN: 0895-3988

www.besjournal.com (full text)

CN: 11-2816/Q

Copyright ©2019 by China CDC

INTRODUCTION

Single high-dose irradiation is performed with stereotactic radiotherapy or occurs in radiation accidents. According to long-term observation, people that undergo

radiotherapy or those that have survived radiation accidents experience an increasing incidence of cardiovascular diseases^[1-2]. Vascular endothelial cells are key cells that mediate radiation-induced cardiovascular diseases^[3-4]. Death and cytokine secretion by the vascular endothelial cells are the

*This study was supported by grants from Research Institute for Social Public Welfare Research Foundation [grant no.2005DIB1J087].

#Correspondence should be addressed to SU Xu, Professor, Tel: 86-10-62389938, Fax: 86-10-62389748, E-mail: suxu@nirp.chinacdc.cn

Biographical note of the first author: LI Chen, female, born in 1987, PhD, Research Assistant, majoring in radiation biology.

main acute effects of radiation-induced injury. These phenomena alter the body milieu causing a systemic chronic inflammatory state, thus leading to age-related disorders such as atherosclerosis and chronic fibrosis^[5]. Therefore, understanding the molecular mechanism of the vascular endothelial cell death pattern induced by single high-dose X-ray is important to limit the side effects of radiotherapy, maximize therapeutic benefits, and improve the quality of life of survivors.

Pyroptosis, a recently reported programmed cell death, could be involved in the death of bone marrow-derived macrophages^[6] and microglia^[7] exposed to radiation. Inhibiting the pyroptosis signaling pathway can alleviate radiation-induced injury of the brain and deterioration of the bone marrow-derived macrophages. However, induction of pyroptosis in the human umbilical vein endothelial cells (HUVECs) by high-dose X-ray and its regulatory mechanism still remain unknown.

Pyroptosis is an inherent inflammatory programmed cell death event that is triggered by various stimuli^[8] such as bacteria, viruses, and toxins^[9]. During pyroptosis, cells initially recognize foreign danger signals, swell, burst, release pro-inflammatory cytokines, and die. Caspase-1 plays an important role during pyroptosis^[8,10-12]. Caspase-1 is activated during pyroptosis by a large supramolecular complex termed inflammasomes^[13-14]. The activated caspase-1 leads to downstream molecules to secrete cytokines and perforates the plasma membrane causing cell burst. Other features of the cells that undergo pyroptosis include swelling and formation of large bubbles on the cell plasma membrane^[9]. Cell death by pyroptosis results in rupture of the plasma membrane and release of damage-associated molecular pattern molecules such as ATP, DNA, and cytokines into the extracellular milieu. These molecules recruit numerous immune cells and initiate the inflammatory cascade in the tissue^[15-16]. However, apoptosis is characterized by packaging of cellular contents and non-inflammatory phagocytic uptake of membrane-bound apoptotic bodies^[9]. So far, no studies have reported high-dose X-ray induced pyroptosis in the HUVECs.

Connexin43 (Cx43) is a transmembrane protein. Its best-known function is to form a gap junction that allows the exchange of molecules that have a size of less than 1.2 kD, such as ions, small molecules, and secondary messengers^[17]. Cx43 exists in various forms, namely, gap junction, hemichannel, or by

itself. This molecule plays an important role in all cell cycle stages such as growth, differentiation, and apoptosis. In the vascular system, the gap junction protein plays a vital role in vascular remodeling^[18], membrane disruption or integrity^[19], and inflammation^[20]. However, the role of Cx43 in mediation of pyroptosis remains unknown.

Pannexin-1 (Panx1) belongs to the Panx family and is also a gap junction protein. However, with respect to Cx43, Panx1 cannot form a gap junction but plays a role as an anion-selective hemichannel during inflammation, apoptosis, and signal transduction. The Panx1 channels open in response to oxygen-glucose deprivation, elevation of $[Ca^{2+}]_i$, and cleavage of C-terminus^[21]. Cleaved Panx1 can form a non-selective channel through the cell membrane and lead to cell death. Thus, a negative correlation possibly exists between Panx1 and Cx43. Moreover, both Panx1 and Cx43 have a similar structure, but have different functions^[22]. A recent study reported that Panx1 is an important mediator of pyroptosis and functions by interacting with the P2X7 receptor^[23-24]. Thus, we assume that Cx43 may regulate pyroptosis by affecting Panx1.

In this study, we used the HUVECs as a model to determine the effect of X-ray. X-ray-induced pyroptosis in the HUVECs decreased the expression of Cx43. We demonstrated that Cx43 modulated pyroptosis in two ways: (1) reversely regulating the activation of the key execution molecule caspase-1, and (2) modulating caspase-1 through the cleaved Panx1-dependent pathway.

MATERIALS AND METHODS

Cell Culture and Irradiation

HUVECs were obtained from the Tumor maker research center (Cancer Hospital Chinese Academy of Medical Sciences, Beijing, China). The HUVECs were maintained in RPMI-1640 medium (Thermo Fisher Scientific, Waltham, MA, USA) supplemented with 10% fetal bovine serum (Thermo Fisher Scientific, Waltham, MA, USA) under a standard condition of 37 °C and 5% CO₂ atmosphere in a humidified incubator.

The cells were inoculated so as to obtain 2×10^5 cells/mL in a 6-well plate or 25 cm² culture flask irradiated at room temperature with 5 Gy/min in a field size of 18 cm × 18 cm and with a source-cell distance of 100 cm by using a 6 MV X-ray source (Elekta Precise Accelerator, Stockholm, Sweden) at

the Huojianjun Hospital. The irradiated HUVECs were washed, resuspended into fresh medium, and placed in to the humidified incubator at 37 °C and 5% CO₂ in a humidified atmosphere. Sham-irradiated HUVECs were used as controls.

Protein Knockdown or Overexpression

For Cx43 knockdown, siRNA: 5'-ACUAGCUGCUG GACAUGAAtt-3' (Cat No. s5757, Thermo Fisher Scientific, Waltham, MA, USA) and LipofectamineTM RNAiMAX (Thermo Fisher Scientific, Waltham, MA, USA) were used according to the manufacturer's instructions. For Panx1 knockdown, siRNA: 5'-GUUUGUGGGAGGUAUCUGAtt-3' (Cat No. s24427, Thermo Fisher Scientific, Waltham, MA, USA) and LipofectamineTM RNAiMAX were used according to the manufacturer's instructions. SilencerTM Select Negative Control No. 1 siRNA (Cat No. 4390843) (Thermo Fisher Scientific, Waltham, MA, USA) was used as a negative control for Cx43 and Panx1 knockdown. For overexpression of Cx43, Biovector NTCC Inc., (Cat No. 597031, Beijing, China) and LipofectamineTM 3000 Transfection Reagent (Thermo Fisher Scientific, Waltham, MA, USA) were used according to the manufacturer's instruction. The pCMV5 plasmid (Cat No. 691965) (Biovector NTCC Inc. Beijing, China) was used as negative control for Cx43 overexpression. Effectiveness of Cx43 knockdown or overexpression was evaluated using western blot analysis.

Western Blot Analysis

HUVECs were lysed in mammalian protein extraction reagent (M-PER) (Thermo Fisher Scientific, Waltham, MA, USA). The lysates were boiled for 8 min, resolved on a 12% SDS-PAGE gel, and transferred onto nitrocellulose membranes (Applygen, Beijing, China). The membranes were blocked with 5% bovine serum albumin (Amresco, OH, USA) in tris-buffered saline solution containing 0.1% (v/v) tween 20 (Thermo Fisher Scientific, Waltham, MA, USA) for 60 min at 25 °C. The antibodies against Cx43, caspase-1, Panx1, and β -tubulin (Cell Signaling Technology, Beverly, MA, USA) were added onto the membranes and the membrane was incubated overnight at 4 °C at dilutions of 1:1,000, 1:1,000, 1:1,000, and 1:2,000, respectively. The immunoblotted membranes were then incubated with horseradish peroxidase-conjugated secondary antibody (ZXBG-Bio, Beijing, China) for 1 h. Immunoreactive

bands were detected using an enhanced chemiluminescence kit (Millipore Corporation, MA, USA).

Analysis of Active Caspase-1 by Fluorescent-labeled Inhibitors of Caspases (FLICA) Staining

FLICA are cell-permeant noncytotoxic probes and covalently bind with active caspase enzymes. Carboxyfluorescein-labeled peptide (Tyr-Val-Ala-Asp)-fluoromethyl ketone (FAM-YVAD-FMK, ImmunoChemistry Technologies, Bloomington, MN, USA) is a FLICA with a preferred binding sequence for caspase-1, and it is used to detect active caspase-1.

The cells were exposed to 10 Gy irradiated or non-irradiated. Approximately 290 μ L of the cell suspension was placed into a fresh tube, and 10 μ L of 30X FLICA was added to it to obtain a final volume of 300 μ L. The solution was mixed by gently flicking the tubes. The cells were then incubated at 37 °C in the dark for 1 h, washed twice with 1X wash buffer, and detected by flow cytometry or confocal microscopy.

For the flow cytometer assay, the cells were resuspended with phosphate buffer saline (PBS) and placed on ice. A 488 nm blue argon laser was used with the emission filter pairing 530/30(FL-1/FITC channel). For each treatment, a minimum of 10,000 cells were analyzed by FACS Calibur (BD, Franklin Lacks, NJ, USA). Data were analyzed using the Cellquest 3.0 software (BD, Franklin Lacks, NJ, USA).

For laser scanning confocal microscopic (Zeiss, Oberkochen, Germany) analysis, the cells were cultivated on a confocal dish by using a bandpass filter excitation of 490 nm and an emission of 530 nm to view green fluorescence. Cells bearing active caspase-1 enzymes that were covalently coupled to FLICA appeared green. The cells were observed with the 40x objective lens.

Transmission Electron Microscopy (TEM)

The specimens were fixed with 2.5% glutaraldehyde (SPI Supplies, PA, USA) in phosphate buffer (pH 7.0) for 3 h, and washed three times in phosphate buffer solution (PBS); post fixation, they were washed with 1% OsO₄ (Ted Pella, CA, USA) in PBS (pH 7.0) for 1 h after which they were washed three times in PBS. The specimens were then dehydrated by a graded series of ethanol (Sigma-Aldrich, MO, USA) (30%, 50%, 70%, 80%, 90%, 95%, and 100%) for 10 min at each step, and transferred to absolute acetone (Sigma-Aldrich, MO,

USA) for 15 min. The specimens were then placed in 1:1 mixture of absolute acetone and the final EPON resin mixture for 1 h at room temperature. It was then transferred to the 1:3 mixture of absolute acetone and the final EPON resin mixture and incubated overnight. The specimens were placed in capsules containing the embedding medium and heated at 37 °C for about 24 h and at 60 °C for about 48 h. Sections of the specimen were stained with uranyl acetate and alkaline lead citrate for 15 min and observed in TEM-Model JEM-1400 PLUS (JEOL, Tokyo, Japan).

Lactate Dehydrogenase Release Assay

Lactate dehydrogenase (LDH) release assay was carried out using the HUVEC culture supernatant by using the LDH Cytotoxicity Assay Kit (Solarbio, China, Beijing) according to the manufacturer's instruction. The cell culture supernatant was collected, centrifuged at 8,000 $\times g$ and 4 °C for 10 min, collected on ice, and 10 μL of the sample was analyzed. OD at 450 nm was detected using the microplate reader Multiskan GO (Thermo Fisher Scientific, Waltham, MA, USA).

Statistical Analysis

Data were presented as mean \pm standard error of the mean (SEM). Statistical analysis for multiple groups was performed using the one-way ANOVA followed by Bonferroni's tests using the GraphPad software (GraphPad Prism, CA, USA). For all statistical analyses, differences were considered to be statistically significant at $P < 0.05$.

RESULTS

High-dose X-ray Induces Pyroptosis in the HUVEC

Active caspase-1 is the hallmark of pyroptosis^[8,10-12]. To confirm whether X-ray induces the death of the HUVECs through pyroptosis, we examined the cleaved caspase-1 (P20) by western blot analysis and FLICA staining (a dye for staining all active forms of caspase-1). After 10 Gy X-ray irradiation, the expression of the cleaved caspase-1 (P20) increased over a period of 6 h up to 48 h (Figure 1A), and in a dose-dependent manner when subjected to different X-ray doses (2.5, 5, 10, and 20 Gy) at 12 h (Figure 1B). FLICA staining (observed using the laser scanning confocal microscope) results showed that the fluorescence intensity in the irradiated group increased compared to that in the non-irradiated group (Figure 1C), indicating higher

expression of the active caspase-1 in the former. The FLICA staining (observed by flow cytometry) (Figure 1D) showed that the percentage of PI⁺-active caspase-1⁺ (represents pyroptotic cells) in the HUVECs from the 10 Gy-irradiated group was significantly higher than that in the control group at 72 h (30.51% \pm 1.99% vs. 2.39% \pm 0.71%, $P < 0.001$). The results obtained using the TEM showed that HUVECs appeared swollen and larger after irradiation (Figure 1E) and exhibited a necrosis-like pattern (typical morphological changes in pyroptotic cells) compared to the non-irradiated group. To evaluate pore formation and cytotoxicity, which are other features of pyroptosis, the LDH release assay was performed in the HUVECs. Pores were formed after 24 h, and a dose-dependent increase in the amount of released LDH was observed (Figure 1F-G). All these results showed that X-ray induced the pyroptosis of HUVECs.

Role of Cx43 in X Ray-induced Pyroptosis of the HUVECs

To understand the role of Cx43 in the HUVECs exposed to X-ray irradiation, we investigated its expression level. The expression of Cx43 in the HUVECs exposed to 10 Gy irradiation decreased from 0 h to 72 h (Figure 2A) in a dose-dependent manner, and was lower than that in the non-irradiated group (Figure 2B).

To confirm the role of Cx43 in mediation of pyroptosis, Cx43 was overexpressed by plasmid transfection and knocked down by RNAi interference. As shown in Figure 3A, the number of PI⁺-active caspase-1⁺ and active caspase-1⁺ HUVECs (representing pro-pyroptotic and pyroptotic cells) decreased in the Cx43 overexpression group (IR-pCMV-Cx43) compared to that in the vector group (IR-pCMV5) (PI⁺-active caspase-1⁺: 22.370% \pm 1.042% vs. 31.917% \pm 0.822%, active caspase-1⁺: 39.740% \pm 1.397% vs. 47.060% \pm 1.215%, $P < 0.01$). The FLICA staining results showed that the fluorescence intensity in the IR-pCMV-Cx43 group decreased compared to that in the IR-pCMV5 group (Figure 3B). The result obtained using western blot analysis (Figure 3C) indicated that the expression of the cleaved caspase-1 (P20) decreased in the IR-pCMV-Cx43 group compared to that in IR-pCMV5 group ($P < 0.01$). Furthermore, the amount of LDH released was lower in the Cx43 overexpression group (Figure 3D) (IR-pCMV-Cx43 vs. IR-pCMV5: 35.748 \pm 1.139 U/mL vs. 44.023 \pm 1.189 U/mL, $P < 0.01$). Thus, overexpression of Cx43 decreased

pyroptosis in the HUVECs by reducing the expression of active caspase-1. However, the number of PI⁺active caspase-1⁺ and active caspase-1⁺ HUVECs in the Cx43 knockdown group (IR-siCx43) increased compared to that in the scramble group (IR-scr) (Figure 4A) (PI⁺active caspase-1⁺: 32.370% ± 1.042% vs. 27.353% ± 2.447%, *P* < 0.05; active caspase-1⁺: 54.773% ± 4.129% vs. 39.740% ± 1.397%, *P* < 0.01). The FLICA staining results showed that the fluorescence intensity in the IR-siCx43 group

increased compared to that in the IR-scr group (Figure 4B). The western blot result (Figure 4C) showed that the expression of the cleaved caspase-1 (P20) increased in the IR-siCx43 group compared to that in IR-scr (*P* < 0.05). The amount of LDH released showed a statistically significant increase in the Cx43 knockdown group (Figure 4D) (IR-siCx43 vs. IR-scr: 54.551 ± 4.014 U/mL vs. 46.652 ± 0.862 U/mL, *P* < 0.05). In addition, HUVECs were swollen, which could lead to cell death (upper panel in Figure 4E), and

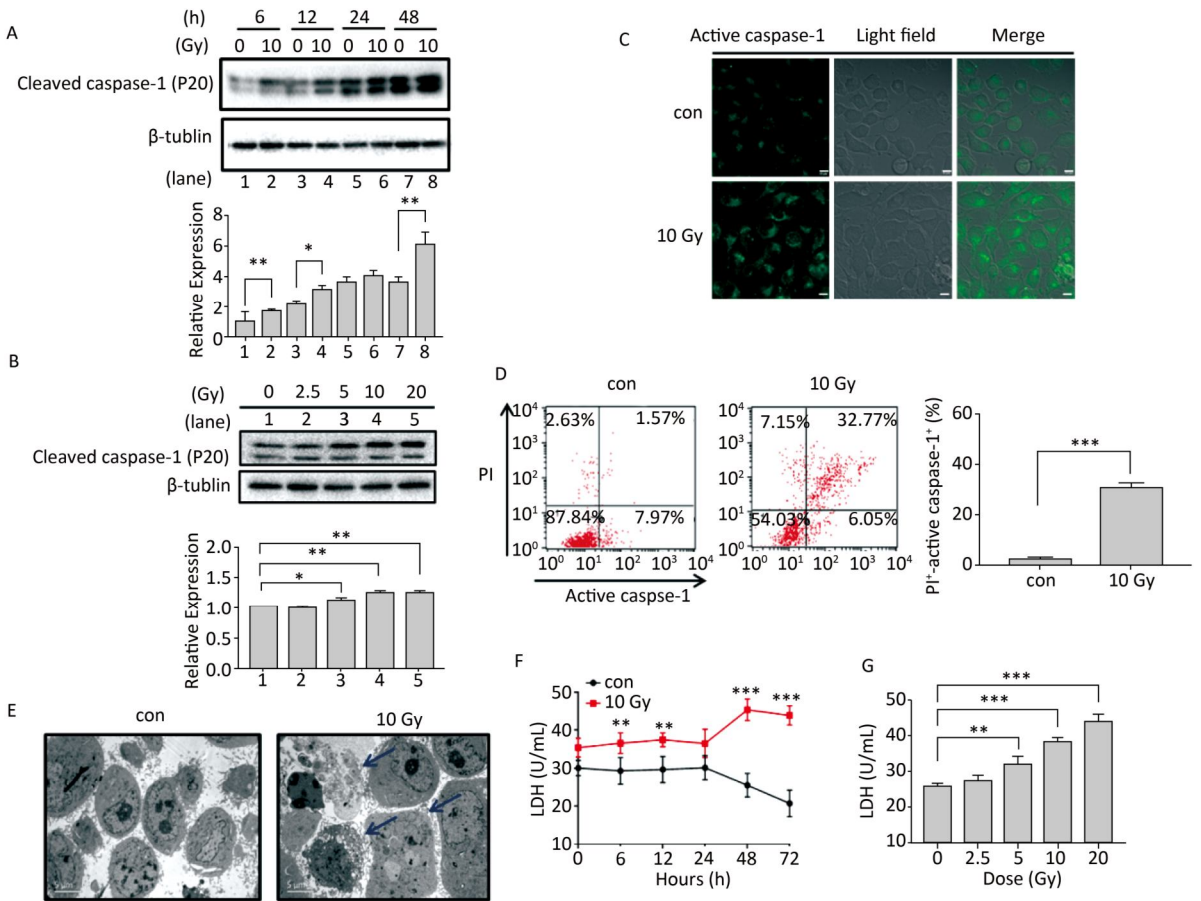


Figure 1. X-ray induces pyroptosis in the HUVECs. (A) Cleaved caspase-1 (P20) was detected after 6 h up to 48 h in the HUVECs after being irradiated with 10 Gy X-ray. (B) Cleaved caspase-1 (P20) was detected in groups subjected to different X-ray doses (2.5, 5, 10, and 20 Gy) at 12 h after irradiation. (C) HUVECs with active caspase-1 (those stained with FLICA appear green) were determined using by confocal microscopy. (D) Percentage of pyroptotic HUVECs was determined with active caspase-1 (those stained with FLICA are represented in the abscissa) and that of PI (represent in ordinate) was determined *via* flow cytometry, and statistical analyses of the percentage of PI⁺active caspase-1⁺ between control (con) and group irradiated with 10 Gy after 72 h are on the right panel. (E) The morphology of the HUVECs was detected by transmission electron microscopy in the control and 10 Gy groups. (F) LDH release was examined at 0-72 h after irradiation and (G) with different doses (2.5, 5, 10, and 20 Gy) at 72 h after irradiation. The results are presented as means ± SEM. Data were obtained from the three independent experiments. Symbols *, **, and *** represent *P* < 0.05, *P* < 0.01, and *P* < 0.001, respectively. Scale bar = 10 μm.

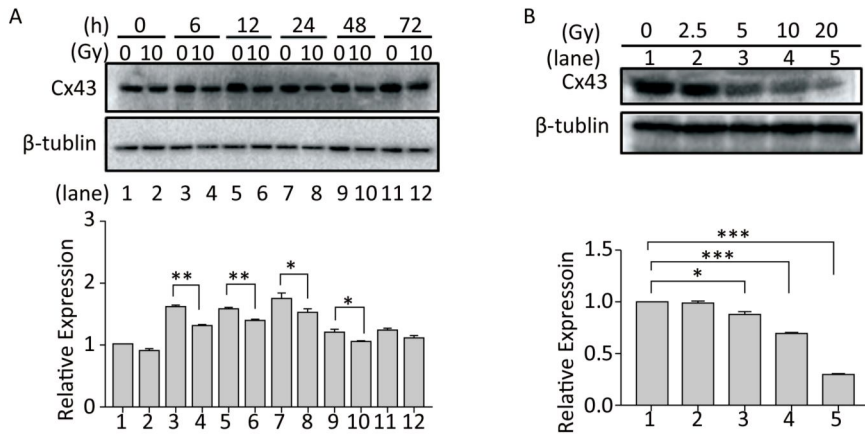


Figure 2. Exposure to X-ray reduces expression of Cx43. (A) Cx43 expression after irradiation with 10 Gy at 0-72 h was detected using western blot analysis. (B) Expression of Cx43 after 12 h of 2.5-10 Gy irradiation as detected by western blot analysis. The results are presented as means \pm SEM. Data were obtained from three independent experiments. Symbols *, **, and *** represent $P < 0.05$, $P < 0.01$, and $P < 0.001$, respectively.

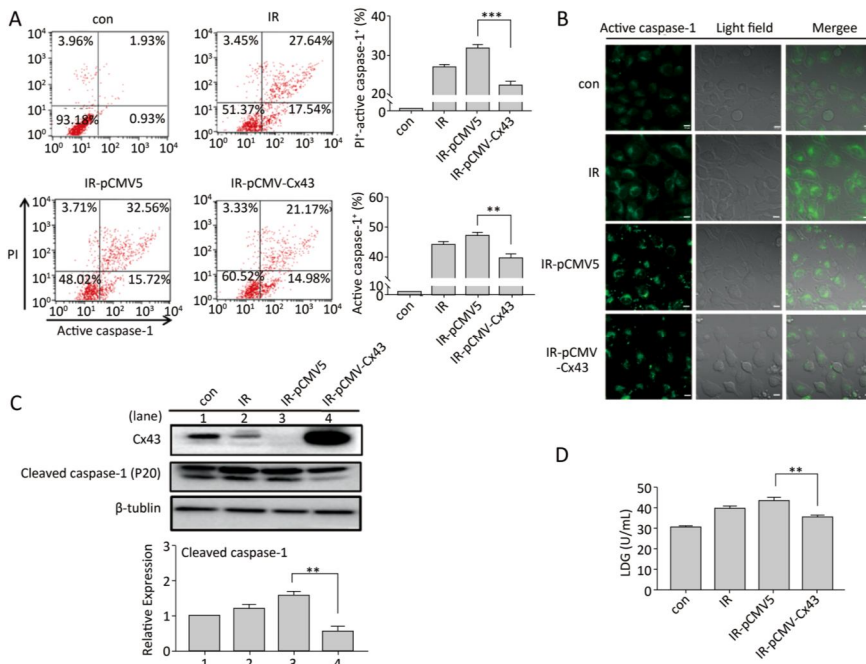


Figure 3. Overexpression of Cx43 decreased pyroptosis in the X-ray-irradiated HUVECs. All the experiments were carried out in the control, irradiation (IR), irradiation with vector (IR-pCMV5), and irradiation with Cx43 overexpression (IR-pCMV-Cx43) groups. (A) Percentage of pyroptotic HUVECs with active caspase-1 (stained with FLICA represented in abscissa) and PI (represented in ordinate) was determined *via* flow cytometry, and statistical analysis of the percentage of PI⁺-active caspase-1⁺ and active caspase-1⁺ HUVECs between the groups after 72 h is presented in the right panel. (B) HUVECs with active caspase-1 (stained with FLICA appear green) were determined using the confocal microscope. (C) Cleaved caspase-1 (P20) and Cx43 were detected at 12 h in HUVECs after irradiation with 10 Gy. (D) The LDH released in the supernatant of each group was examined. The results are presented as means \pm SEM. Data was obtained from three independent experiments. Symbols ** and *** represent $P < 0.01$ and $P < 0.001$, vs. IR-pCMV5, respectively. Scale bar = 10 μ m.

the number of vesicles, which could be inflammasomes, between cell membranes increased (under panel in Figure 4E). Thus, Cx43 knockdown enhanced pyroptosis in the HUVECs by elevating active caspase-1.

Cx43 Mediates Pyroptosis by Affecting Cleaved Panx1

Cleaved Panx1 is an important factor that influences pyroptosis by interacting with the P2X7 receptor^[23-24]. After X-ray irradiation, expression of the

cleaved Panx1 increased after 12 h to 72 h compared to that in the non-irradiated group (Figure 5A), and the increase was dose-dependent from 0-10 Gy (Figure 5B). To determine the role of Cx43 in regulating cleaved Panx1, Cx43 was overexpressed and knocked down in the irradiated HUVECs. Cx43 overexpression decreased the expression of cleaved Panx1 ($P < 0.01$, Figure 5C), whereas Cx43 knockdown increased the expression ($P < 0.05$, Figure 5D). Hence, Cx43 mediated formation of cleaved Panx1 in irradiated HUVECs.

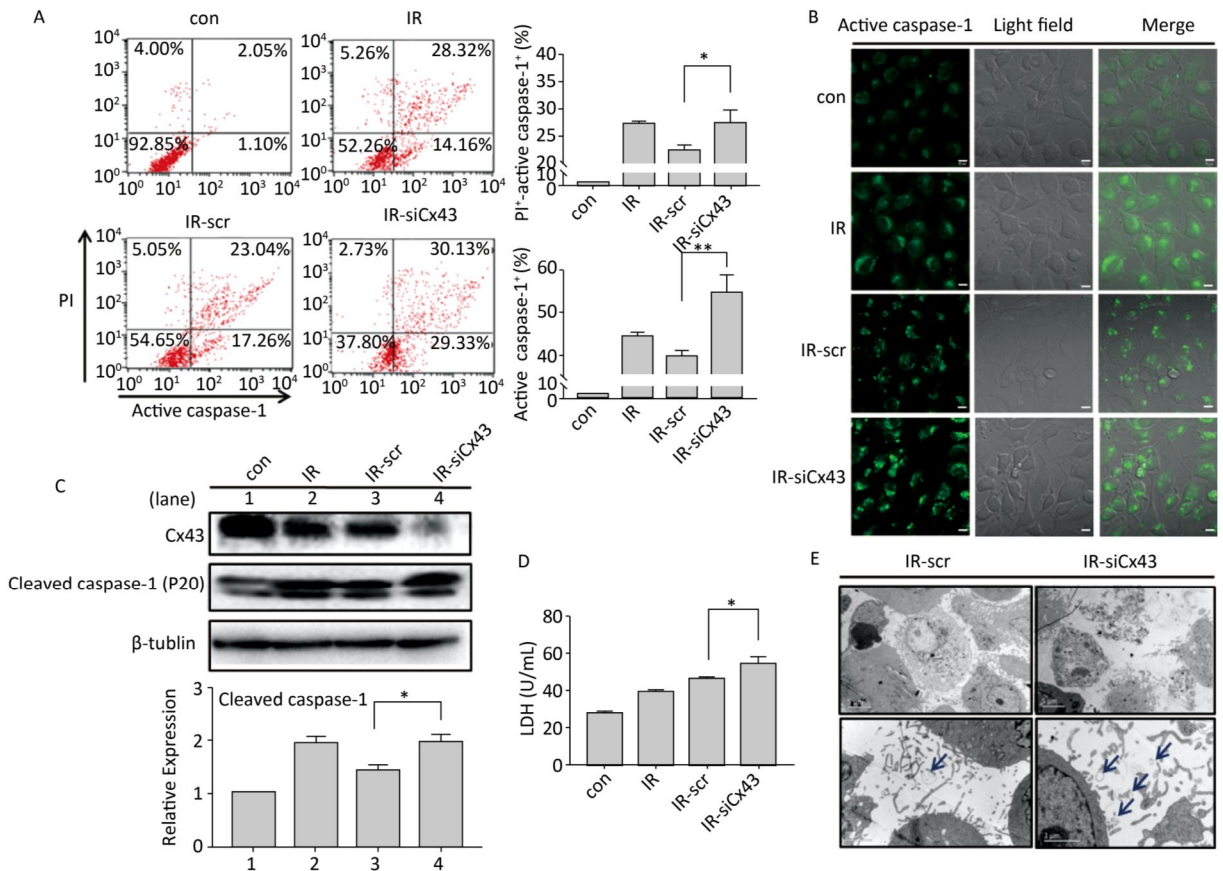


Figure 4. Cx43 knockdown increases pyroptosis in the X-ray-irradiated HUVECs. All the experiments were carried out in the control, irradiation (IR), irradiation with scramble (IR-scr), and irradiation with Cx43 knockdown (IR-siCx43) groups. (A) Percentage of pyroptotic HUVECs was determined with active caspase-1 (stained with FLICA represent in abscissa) and PI (represent in ordinate) *via* flow cytometry, and statistical analysis of the percentage of PI⁺-active caspase-1⁺ and active caspase-1⁺ HUVECs between groups after 72 h is presented in the right panel. (B) HUVECs with active caspase-1 (stained with FLICA appear green) were determined by confocal microscopy. (C) Cleaved caspase-1 (P20) and Cx43 were detected at 12 h in HUVECs after irradiation with 10 Gy. (D) LDH release from the supernatant of each group. (E) Morphology of HUVECs transfected with vector scr or siCx43 irradiated with 10 Gy after 72 h, as detected by transmission electron microscopy. The results are presented as means ± SEM. Data were obtained from three independent experiments. Symbols * and ** represent $P < 0.05$ and $P < 0.01$, vs. IR-scr, respectively. Scale bar = 10 μm.

To determine if Panx1 regulates X ray-induced pyroptosis, the percentage of PI⁺-active caspase-1⁺ and active caspase-1⁺ HUVECs with or without Panx1 knockdown was examined by flow cytometry analysis. As shown in Figure 6A, the number of PI⁺-active caspase-1⁺ and active caspase-1⁺ HUVECs in the Panx1 knockdown group (IR-siPanx1) decreased compared to that in the IR-scr group (PI⁺-active caspase-1⁺: IR-siPanx1 vs. IR-scr: 14.637% ± 0.391% vs. 22.370% ± 1.042%, $P < 0.001$; active caspase-1⁺: IR-siPanx1 vs. IR-scr: 18.400% ± 0.104% vs. 39.740% ± 1.397%, $P < 0.001$). Expression of the cleaved caspase-1 in IR-siPanx1 decreased compared with that in IR-scr ($P < 0.05$, Figure 6C). The LDH release assay (Figure 6D) indicated that IR-siPanx1 HUVECs displayed less cytotoxicity than IR-scr (IR-siPanx1 vs. IR-scr: 40.881 ± 1.435 U/mL vs. 50.888 ± 1.758 U/mL; $P < 0.01$). Thus, Panx1 could play an important role in

the regulation of X-ray-induced pyroptosis.

We speculated whether Cx43 mediates pyroptosis through cleaved Panx1. We knocked down Cx43 and Panx1 simultaneously to determine whether the role of Cx43 in pyroptosis was negatively affected. As shown in Figure 6A, the percentage of PI⁺-active caspase-1⁺ HUVECs in the double-knockdown group (IR-siCx43-siPanx1) was lower than that in the IR-siCx43 group (25.047% ± 1.819% vs. 27.353% ± 2.447%). The percentage of active caspase-1⁺ in IR-siCx43-siPanx1 significantly decreased compared to that in the IR-siCx43 (41.060% ± 0.98% vs. 54.773% ± 4.129%, $P < 0.01$) group. Hence, Cx43 could regulate the cleaved Panx1 to mediate the initial stages of pyroptosis. The FLICA staining results also showed that the fluorescence intensity in the IR-siCx43-siPanx1 group decreased compared to that in the IR-siCx43 group (Figure 6B).

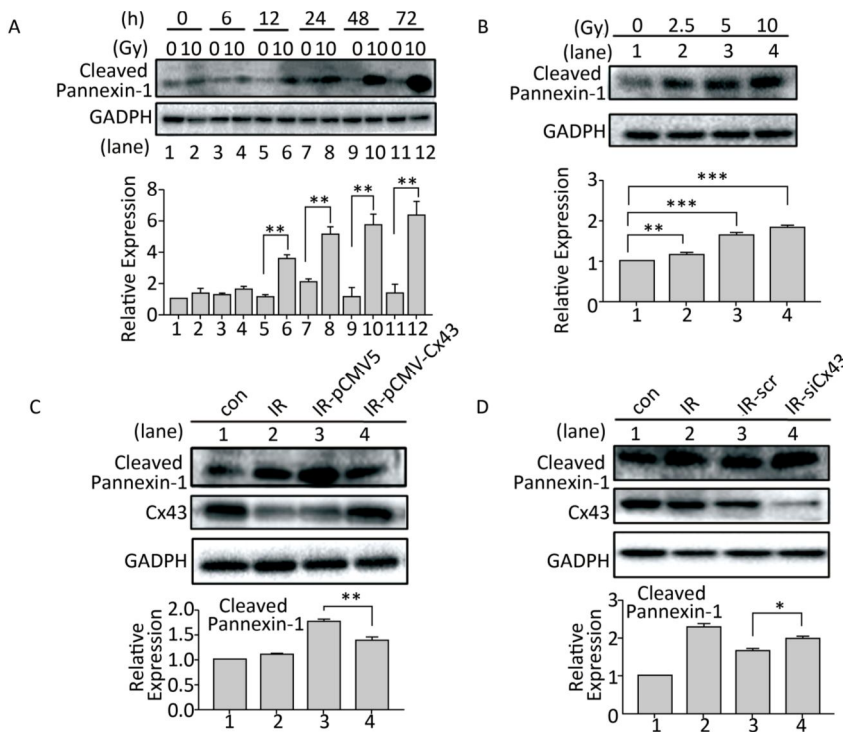


Figure 5. Cx43 affects Pannexin-1 in X-ray-irradiated HUVECs. (A) Cleaved Pannexin-1 was detected between 0-72 h in HUVECs after irradiated by 10 Gy X-ray. (B) Cleaved Pannexin-1 expression level in HUVECs after 0, 2.5, 5, 10, and 20 Gy radiation at 12 h. (C) Cleaved Pannexin-1 and Cx43 expression in HUVECs after 10 Gy radiation at 12 h in control, irradiation (IR), irradiation with vector (IR-pCMV5), and irradiation with Cx43 overexpression (IR-pCMV-Cx43) groups. (D) Cleaved Pannexin-1 and Cx43 expression in HUVECs after 10 Gy radiation at 12 h in control, irradiation (IR), irradiation with scramble (IR-scr), and irradiation with Cx43 knockdown (IR-siCx43) groups. The results are presented as means ± SEM. Data were obtained from three independent experiments. Symbols *, **, and *** represent $P < 0.05$, $P < 0.01$, and $P < 0.001$, respectively.

As shown in Figure 6C, Cx43 and Panx1 knockdown significantly inhibited Cx43 knockdown-induced elevation of cleaved caspase-1 (P20) ($P < 0.001$). Moreover, the LDH release assay showed that the double-knockdown group displayed less cytotoxicity

than the single Cx43 knockdown group (52.598 ± 2.067 U/mL vs. 65.174 ± 4.388 U/mL, $P < 0.05$).

Overall, evidence indicates that Cx43 modulates pyroptosis directly by regulating the active caspase-1 and by mediating the expression of cleaved Panx1.

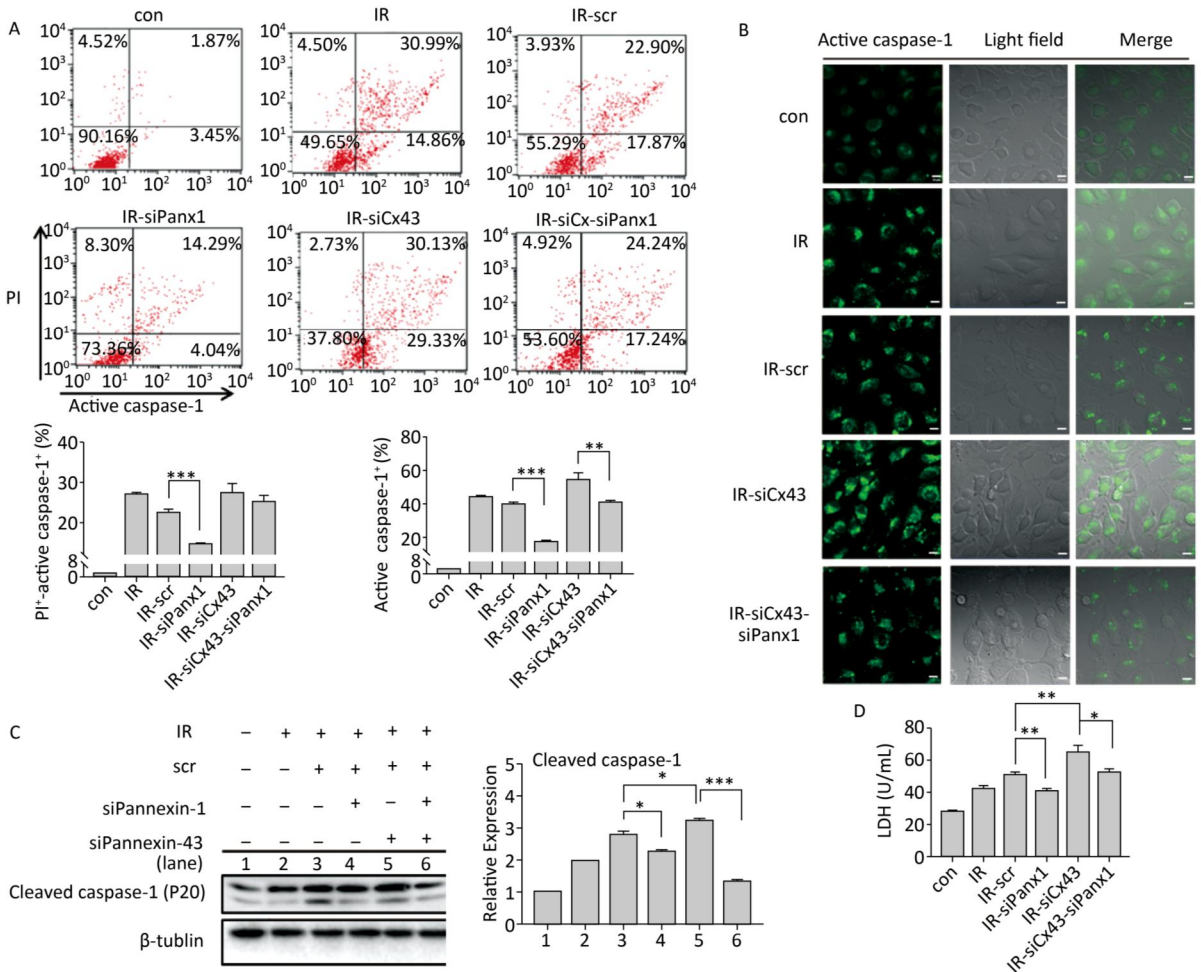


Figure 6. Cx43 mediates pyroptosis through cleaved Pannexin1. All the experiments were carried out in the control, irradiation (IR), irradiation with scramble (IR-scr), irradiation with Panx1 knockdown (IR-siPanx1), irradiation with Cx43 knockdown (IR-siCx43), and irradiation with both Cx43 knockdown and Panx1 knockdown (IR-siCx43-siPanx1). (A) Percentage of pyroptotic HUVECs was determined with active caspase-1 (stained with FLICA represent in abscissa) and PI (represent in ordinate) *via* flow cytometry, and statistical analysis of percentage of PI⁺-active caspase-1⁺ and active caspase-1⁺ HUVECs between groups after 72 h is presented in the right panel. (B) HUVECs with active caspase-1 (stained with FLICA appear green) were determined *via* confocal microscopy. (C) Cleaved caspase-1 (P20) was detected using western-blot analysis at 12 h after 10 Gy X-ray irradiation in each group. (D) LDH release from the supernatant of each group was examined by the LDH release assay. The results are presented as means \pm SEM. Data was obtained from three independent experiments. Symbols *, **, and *** represent $P < 0.05$, $P < 0.01$, and $P < 0.001$ respectively. Scale bar = 10 μ m.

DISCUSSION

After radiotherapy or radiation accidents, the ionizing radiations cause vascular endothelium damage, resulting in platelet aggregation, inflammation, and vascular remodeling, followed by reduced vascular density, ischemia, and fibrosis^[25]. Vascular endothelial cells have gained immense attention in the field of radiation protection^[26]. The present study aimed to determine whether X-ray could induce pyroptosis in the HUVECs, identify the role of Cx43 in regulating this process, and establish the underlying mechanism. Apoptosis was originally thought to play a predominant role in radiation-induced cell injury; however, based on our observation, HUVECs exposed to X-ray showed a different type of death, namely, pyroptosis, in the early stage. Pyroptosis is a highly inflammatory form of programmed cell death and could play an important role in injuries caused by X-ray. Understanding the molecular pathways of radiation-induced pyroptosis in the HUVECs might help understand the mechanism of the side effects of X-ray on normal tissues. This study is the first to demonstrate this type of cell death during vascular endothelial injury induced by X-ray. The results may provide a new perspective in understanding cell death induced by X-ray.

In this study, our hypothesis is confirmed by the following observations. (i) The expression of cleaved caspase-1 (P20), a molecular marker of pyroptosis, gradually increased from 6 h to 48 h in the 10 Gy-irradiated group than in the non-irradiated group. (ii) The percentage of PI⁺-active caspase-1⁺ HUVECs was higher at 72 h after 10 Gy than in the non-irradiated group. (iii) Analysis using TEM and the LDH release assay results showed swelling and bursting of HUVECs at 72 h after 10 Gy irradiated. Other researchers have also found that radiation could induce pyroptosis; however, such studies were carried out using different radiation doses and cell types^[6-7,27-28]. We also found that at 72 h after 10 Gy irradiation, the expression of active caspase-1 (P20) decreased, and that of cleaved caspase-3 increased (data not shown). Hence, whether the cell death way transfer from pyroptosis to apoptosis or only pyroptosis (because cleaved caspase-3 is induced by active caspase-1) must be further confirmed; this phenomenon was named by some scholars as pyrop-apoptosis^[10].

Cx43 affects apoptosis in different cell types in response to various stimuli^[29-31]; however, whether

Cx43 influences pyroptosis and the underlying mechanism remain unknown. Research in radiation-related field indicates that Cx43 is associated with inflammation, membrane permeability, hypersensitivity, and the bystander effect. For radiation-induced expression of Cx43, studies at different laboratories and using different radiation types and cells showed variable results^[32-34]. Variation with respect to the radiation source, radiation dose, cell type, cell sensitivity, or injury type may result in different expression profiles^[35]. In the present study, we found that X-ray dose-dependently decreased the Cx43 expression from 0 h to 72 h. We also found the phosphorylation level of Ser368, an indicator of Cx43 degradation, increased (unpublished data in a separate manuscript), thereby confirming X-ray decreased Cx43 expression and X-ray irradiation disturbed the upstream of Cx43 probably through the PKC pathway^[36].

To identify and improve our current understanding of the role of Cx43 during pyroptosis, Cx43 was overexpressed. Our data indicated that overexpression of Cx43 prevented cell death by decreasing the active caspase-1 expression and the amount of LDH released. In addition, Cx43 knockdown deteriorated cell's condition. Therefore, the Cx43-associated pathway possibly contributes significantly to X-ray-induced pyroptosis by directly acting on caspase-1. Reports have shown that Cx43 regulates intracellular Ca²⁺ signal^[37-38]. Moreover, the Ca²⁺ signaling pathway could regulate the activation of the inflammasome^[39-41] (upstream of caspase-1 activation). Thus, the biological mechanism of Cx43 affecting caspase-1 is probably by modulating Ca²⁺ signal.

Interestingly, in our experiment, X-ray increased the expression of cleaved Panx1 from 12 h to 72 h after irradiation and in a dose dependent manner at 12 h but decreased that of Cx43. A negative correlation possibly exists between the two proteins. Other reports showed that Panx1 and Cx43 are structurally similar, but have different functions^[22]. Thus, we assume that the X ray-irradiated HUVECs led to downregulation of Cx43, resulting in the upregulation of cleaved-Panx1. Moreover, Panx1 plays a vital role in regulating pyroptosis by modulating the efflux of ATP and K⁺ by interacting with the P2X7 receptor^[42-46]. The level of cleaved Panx1 represents the open and active states of Panx1. Hence, Cx43 may modulate pyroptosis *via* a cleaved Panx1-dependent pathway.

Our results showed that Cx43 knockdown significantly elevates the expression of active caspase-1, but at the same time, Panx1 knockdown downregulates active caspase-1. Hence, cleaved Panx1 is located downstream of Cx43. In addition, Panx1 and Cx43 are structurally similar, but they have different ancestor genes and functions. We speculate if X-ray affects a gene that transfers Cx43 to Panx1 and eventually leads to pyroptosis. This presumption must be further explored. Recent reports have shown that Cx43 can influence the upstream of caspase-1 to

regulate pyroptosis^[47-48]. Other studies indicated that Cx43 can mediate the downstream of pyroptosis, such as ATP release^[49]. We mentioned above that Panx1 can modulate ATP by interacting with the P2X7 receptor. Hence, the latter report indirectly proved our findings in the experiment.

In summary, this study supports a rational new pathway for explaining X-ray-induced injury in the HUVECs (as shown in Figure 7). Further studies are required to explore the potential of Cx43 to reduce damage to the HUVECs.

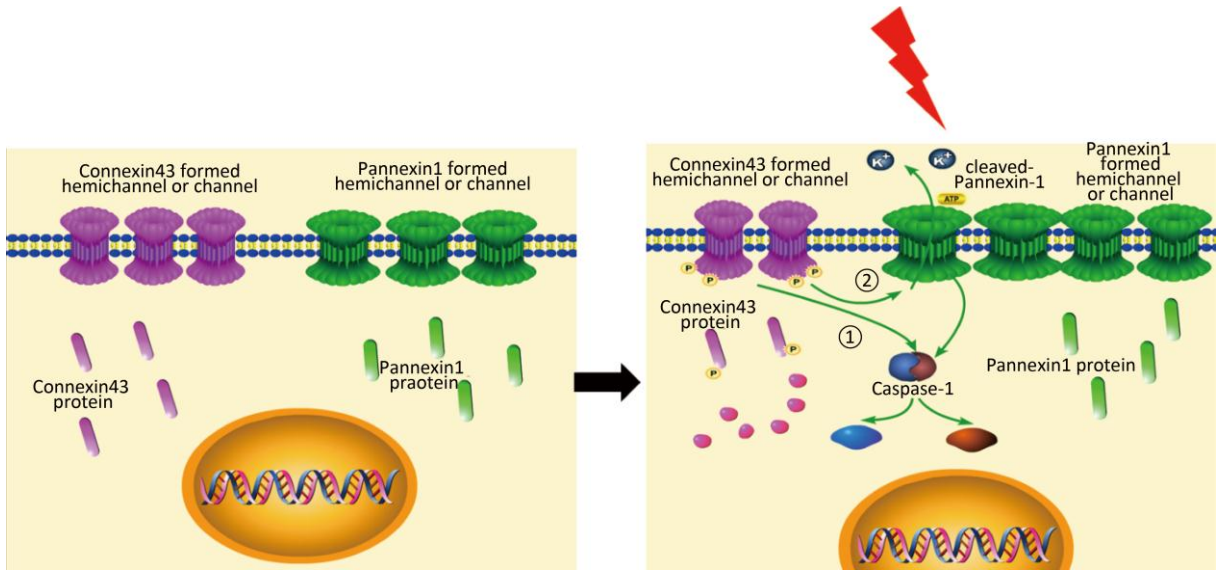


Figure 7. Schematic diagram of Cx43 regulating X-ray-irradiated HUVECs pyroptosis. ①The direct way in which Cx43 modulates the X-ray-irradiated HUVECs pyroptosis through caspase-1 ②The indirect way in which Cx43 modulates X-ray-irradiated HUVECs pyroptosis through cleaved-Pannexin-1.

Received: November 16, 2018;

Accepted: February 19, 2019

REFERENCES

- Formenti SC, Lymeris SC, Dewyngaert JK. Ischemic heart disease after breast cancer radiotherapy. *N Engl J Med*, 2013; 368, 2525.
- Shimizu Y, Kodama K, Nishi N, et al. Radiation exposure and circulatory disease risk: Hiroshima and Nagasaki atomic bomb survivor data, 1950-2003. *BMJ*, 2010; 340, b5349.
- Korpela E, Liu SK. Endothelial perturbations and therapeutic strategies in normal tissue radiation damage. *Radiat Oncol*, 2014; 9, 1-9.
- Corre I, Guillonnet M, Paris F. Membrane signaling induced by high doses of ionizing radiation in the endothelial compartment. Relevance in radiation toxicity. *Int J Mol Sci*, 2013; 14, 22678-96.
- Venkatesulu BP, Mahadevan LS, Aliru ML, et al. Radiation-Induced Endothelial Vascular Injury: A Review of Possible Mechanisms. *JACC Basic Transl Sci*, 2018; 3, 563-72.
- Liu YG, Chen JK, Zhang ZT, et al. NLRP3 inflammasome activation mediates radiation-induced pyroptosis in bone marrow-derived macrophages. *Cell Death Dis*, 2017; 8, e2579.
- Liao H, Wang H, Rong X, et al. Mesenchymal stem cells attenuate radiation-induced brain injury by inhibiting microglia pyroptosis. *Biomed Res Int*, 2017; 2017, 1948985.
- Bergsbaken T, Fink SL, Cookson BT. Pyroptosis: host cell death and inflammation. *Nat Rev Microbiol*, 2009; 7, 99-109.
- Shi J, Gao W, Shao F. Pyroptosis: Gasdermin-mediated programmed necrotic cell death. *Trends Biochem Sci*, 2017; 42, 245-54.
- Xi H, Zhang Y, Xu Y, et al. Caspase-1 inflammasome activation mediates homocysteine-induced pyrop-apoptosis in endothelial cells. *Circ Res*, 2016; 118, 1525-39.
- Abe J, Morrell C. Pyroptosis as a regulated form of necrosis: PI^+ /Annexin V/High Caspase 1/Low Caspase 9 activity in cells = pyroptosis? *Circ Res*, 2016; 118, 1457-60.
- Miao EA, Leaf IA, Treuting PM, et al. Caspase-1-induced pyroptosis is an innate immune effector mechanism against intracellular bacteria. *Nat Immunol*, 2010; 11, 1136-42.
- Lamkanfi M, Dixit VM. Mechanisms and functions of inflammasomes. *Cell*, 2014; 157, 1013-22.

14. Schroder K, Tschopp J. The inflammasomes. *Cell*, 2010; 140, 821-32.
15. Franklin BS, Bossaller L, De Nardo D, et al. The adaptor ASC has extracellular and 'prionoid' activities that propagate inflammation. *Nat Immunol*, 2014; 15, 727-37.
16. Baroja-Mazo A, Martín-Sánchez F, Gomez AI, et al. The NLRP3 inflammasome is released as a particulate danger signal that amplifies the inflammatory response. *Nat Immunol*, 2014; 15, 738.
17. Skerrett IM, Williams JB. A structural and functional comparison of gap junction channels composed of connexins and innexins. *Dev Neurobiol*, 2017; 77, 522-47.
18. Dempsie Y, Martin P, Upton PD. Connexin-mediated regulation of the pulmonary vasculature. *Biochem Soc Trans*, 2015; 43, 524-9.
19. Zhang J, O'Carroll SJ, Henare K, et al. Connexin hemichannel induced vascular leak suggests a new paradigm for cancer therapy. *FEBS Lett*, 2014; 588, 1365-71.
20. De Bock M, Wang N, Decrock E, et al. Intracellular cleavage of the Cx43 c-terminal domain by matrix-metalloproteases: A novel contributor to inflammation? *Mediat Inflamm*, 2015; 2015, 1-18.
21. Taylor KA, Wright JR, Mahaut-Smith MP. Regulation of pannexin-1 channel activity. *Biochem Soc Trans*, 2015; 43, 502-7.
22. Thi MM, Islam S, Suadicani SO, et al. Connexin43 and pannexin-1 channels in osteoblasts: who is the "hemichannel"? *J Membr Biol*, 2012; 245, 401-9.
23. Li S, Tomic M, Stojilkovic SS. Characterization of novel pannexin 1 isoforms from rat pituitary cells and their association with ATP-gated P2X channels. *Gen Comp Endocrinol*, 2011; 174, 202-10.
24. Pelegrin P, Surprenant A. Pannexin-1 mediates large pore formation and interleukin-1beta release by the ATP-gated P2X7 receptor. *EMBO J*, 2006; 25, 5071-82.
25. Rafii S, Ginsberg M, Scandura J, et al. Transplantation of Endothelial Cells to Mitigate Acute and Chronic Radiation Injury to Vital Organs. *Radiat Res*, 2016; 186, 196-202.
26. Slezak J, Kura B, Ravingerova T, et al. Mechanisms of cardiac radiation injury and potential preventive approaches. *Can J Physiol Pharmacol*, 2015; 93, 737-53.
27. Wu D, Han R, Deng S, et al. Protective effects of flagellin A N/C against radiation-induced NLR Pyrin domain containing 3 inflammasome-dependent pyroptosis in Intestinal Cells. *Int J Radiat Oncol Biol Phys*, 2018; 101, 107-17.
28. Han R, Wu D, Deng S, et al. NLRP3 inflammasome induces pyroptosis in lung tissues of radiation-induced lung injury in mice. *Chinese J Cell & Mol Immunol*, 2017; 33, 1206-11. (In Chinese)
29. Pecoraro M, Pinto A, Popolo A. Inhibition of connexin 43 translocation on mitochondria accelerates CoCl₂-induced apoptotic response in a chemical model of hypoxia. *Toxicol In Vitro*, 2018; 47, 120-8.
30. Du ZJ, Cui GQ, Zhang J, et al. Inhibition of gap junction intercellular communication is involved in silica nanoparticles-induced H9c2 cardiomyocytes apoptosis via the mitochondrial pathway. *Int J Nanomedicine*, 2017; 12, 2179-88.
31. Ghosh S, Kumar A, Chandna S. Connexin-43 downregulation in G2/M phase enriched tumour cells causes extensive low-dose hyper-radiosensitivity (HRS) associated with mitochondrial apoptotic events. *Cancer Lett*, 2015; 363, 46-59.
32. Mathur A, Kumar A, Babu B, et al. *In vitro* mesenchymal-epithelial transition in NIH3T3 fibroblasts results in onset of low-dose radiation hypersensitivity coupled with attenuated connexin-43 response. *Biochim Biophys Acta Gen Sub*, 2018; 1862, 414-26.
33. Autsavapromporn N, de Toledo SM, Little JB, et al. The role of gap junction communication and oxidative stress in the propagation of toxic effects among high-dose alpha-particle-irradiated human cells. *Radiat Res*, 2011; 175, 347-57.
34. Azzam EI, de Toledo SM, Little JB. Expression of connexin43 is highly sensitive to ionizing radiation and other environmental stresses. *Cancer Res*, 2003; 63, 7128-35.
35. Autsavapromporn N, De Toledo SM, Jay-Gerin JP, et al. Human cell responses to ionizing radiation are differentially affected by the expressed connexins. *J Radiat Res*, 2013; 54, 251-9.
36. Lampe PD, Tenbroek EM, Burt BJM, et al. Phosphorylation of connexin43 on serine368 by protein kinase C regulates gap junctional communication. *J Cell Biol*, 2000; 149, 1503-12.
37. Decrock E, Hoorelbeke D, Ramadan R, et al. Calcium, oxidative stress and connexin channels, a harmonious orchestra directing the response to radiotherapy treatment? *Biochim Biophys Acta Mol Cell Res*, 2017; 1864, 1099-120.
38. Li C, Meng Q, Yu X, et al. Regulatory effect of connexin 43 on basal Ca²⁺ signaling in rat ventricular myocytes. *PLoS One*, 2012; 7, e36165.
39. Lee GS, Subramanian N, Kim AI, et al. The calcium-sensing receptor regulates the NLRP3 inflammasome through Ca²⁺ and cAMP. *Nature*, 2012; 492, 123-7.
40. Chang YY, Kao MC, Lin JA, et al. Effects of MgSO₄ on inhibiting Nod-like receptor protein 3 inflammasome involve decreasing intracellular calcium. *J Surg Res*, 2018; 221, 257-65.
41. Gong T, Yang Y, Jin T, et al. Orchestration of NLRP3 Inflammasome Activation by Ion Fluxes. *Trends Immunol*, 2018; 39, 393-406.
42. Crespo YS, Willebrords J, Johnstone SR, et al. Pannexin1 as mediator of inflammation and cell death. *Biochim Biophys Acta Mol Cell Res*, 2017; 1864, 51-61.
43. Draganov D, Gopalakrishnapillai S, Chen YR, et al. Modulation of P2X₄/P2X₇/Pannexin-1 sensitivity to extracellular ATP via Ivermectin induces a non-apoptotic and inflammatory form of cancer cell death. *Sci Rep*, 2015; 5, 16222.
44. deGassart A, Martinon F. Pyroptosis: Caspase-11? Unlocks the gates of death. *Immunity*, 2015; 43, 835-7.
45. Qu Y, Misaghi S, Newton K, et al. Pannexin-1 is required for ATP release during apoptosis but not for inflammasome activation. *J Immunol*, 2011; 186, 6553-61.
46. Richter K, Kiefer KP, Grzesik BA, et al. Hydrostatic pressure activates ATP-sensitive K⁺ channels in lung epithelium by ATP release through pannexin and connexin hemichannels. *FASEB J*, 2014; 28, 45-55.
47. Tonkin RS, Bowles C, Perera CJ, et al. Attenuation of mechanical pain hypersensitivity by treatment with Peptide5, a connexin-43 mimetic peptide, involves inhibition of NLRP3 inflammasome in nerve-injured mice. *Exp Neurol*, 2018; 300, 1-12.
48. Mugisho OO, Green CR, Kho DT, et al. The inflammasome pathway is amplified and perpetuated in an autocrine manner through connexin43 hemichannel mediated ATP release. *Biochim Biophys Acta Gen Subj*, 2018; 1862, 385-93.
49. Lohman AW, Isakson BE. Differentiating connexin hemichannels and pannexin channels in cellular ATP release. *FEBS Letters*, 2014; 588, 1379-88.